Innovative: International Multi-disciplinary Journal of Applied Technology
(ISSN 2995-486X) VOLUME 04 ISSUE 04, 2026

MATHEMATICAL MODELING OF THERMAL PROCESSES IN TRUNCATED CONICAL SOLAR WATER HEATERS

N.R. Esanaliyeva
Department of Electronics and Instrument Engineering
Fergana State Technic Universery
Fergana, Uzbekistan

Abstract:
This article examines the mathematical modeling of thermal processes occurring in a truncated conical solar water heater collector. These collectors are crucial in enhancing energy efficiency and developing environmentally friendly heat sources. During the modeling process, convection, heat conduction, and radiative heat transfer processes are clearly expressed based on the Navier-Stokes equations. The complex nature of heat flow, the geometric characteristics of the collector, and the non-uniform absorption of solar radiation are all taken into account in the model. A three-dimensional system of differential equations, which describes the conservation of mass, momentum, and energy transfer, is used as the basis of the mathematical model. Also, the correct definition of boundary and initial conditions ensures that thermal processes are modeled in accordance with real conditions. The results of this study have served to increase the efficiency of solar water heater collectors and provide a deep analysis of heat exchange processes.

Keywords: solar radiation, absorber, energy efficiency, truncated conical solar water heater

1. Introduction

It is well known that natural fuel and energy resources, which are currently used on an industrial scale, are gradually decreasing. Therefore, the use of renewable energy sources allows for the preservation of natural resources and the ecological situation at their current levels [1]. This is because in the 21st century, the world faces two serious problems in the energy sector: ensuring a reliable energy supply and combating climate change [2-3]. The growing environmental problems, on one hand, and the highly unstable energy market, on the other, as well as the risks of an energy supply system if it is solely based on the use of fuel, will lead to serious energy resource problems in the future, considering that any type of resource is a finite one. Currently, due to the inherent difficulties in producing thermal energy, it is one of the most expensive types of energy. Furthermore, due to high fuel prices and the low efficiency of thermal power plants, the efficiency of the heat supply process to consumers is approximately 40-70% [4].

Rapid global growth in energy demand together with declining supplies of fossil fuels has increased the need for sustainable, renewable energy. Over the past few decades total world primary energy consumption has risen by more than 30%, while renewables have increased only modestly. This underlines the urgency of faster deployment of clean technologies [5-

6].Solar thermal energy, in particular for space and industrial heating needs, can be considered one of the most promising and environmentally applicable methods [7-8].

Solar radiation received at Earth can be converted, directly or indirectly, into other energy forms such as heat and electricity [9]. Only a tiny fraction of the Sun's emitted energy reaches Earth — about one two-billionth, i.e., 1.15×10^19 J/min. Of the solar energy that reaches the Earth's atmosphere, roughly 40% is reflected back to space by the atmosphere, about 16% is absorbed by the atmosphere, and the remainder passes through the atmosphere to reach the Earth's surface [10]. For this reason, solar-energy-based renewable technologies are being developed on our planet.

Among renewable technologies, solar water heating systems (SWH) stand out for their ability to convert solar irradiation directly into useful thermal energy with minimal conversion losses [11]. Studies show that in both developing and developed countries, 40% to 60% of household thermal energy demand is used for water heating [12]. Consequently, integrating solar water heating technologies into residential and commercial buildings can substantially reduce energy consumption from conventional sources and cut greenhouse gas emissions [13].

Moreover, designing and installing solar water heaters is generally straightforward, and they can operate independently of centralized energy systems, making them especially attractive for rural and low-density areas [14]. Their maintenance requirements are relatively low compared with photovoltaic or wind systems, which improves their economic viability. The International Energy Agency (IEA) estimated that global installed solar thermal capacity exceeded 500 GW by 2023, resulting in a significant reduction in CO2 emissions worldwide 12.

From the perspective of sustainable development, solar water heating is directly tied to affordable and clean energy and indirectly to mitigating climate change by reducing reliance on fossil-fuel-based water heating [15]. Awareness of energy efficiency, government incentives, and reductions in production costs for solar collectors are likely to further accelerate the deployment of these systems in many regions such as Asia, Africa, and Latin America [16].

Uzbekistan's geographic conditions provide favorable solar energy resources, with an annual average of 2,800–3,100 sunshine hours and an average daily solar irradiation of approximately 4.5–6.0 kW/m^2 [17].

Fig.1 shows the average annual solar radiation measured in various regions of Uzbekistan, expressed in kilowatt-hours per square meter (kWh/m^2).

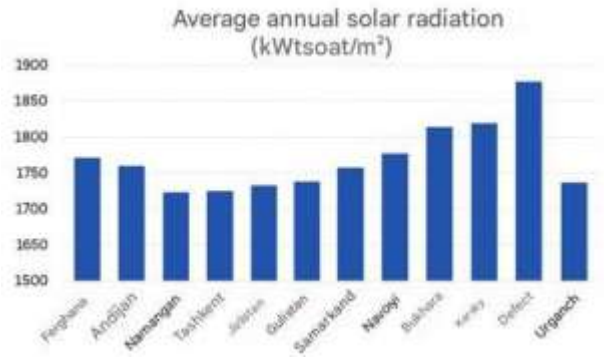

Figure 1. Average annual solar radiation in various regions of Uzbekistan

The highest annual solar radiation is observed in the city of Nukus, with a value of approximately 1900 kWh/m^2. This makes the region one of the most favorable locations for solar energy projects.

The city of Termez also records high solar radiation, slightly lower than Nukus. Therefore, this area is also considered promising for efficient use of solar energy.

The lowest average annual radiation is found in the Andijan, Namangan, and Tashkent regions, with Namangan having the least solar radiation among them. This suggests that solar energy projects in these areas may be less efficient compared to those in Nukus or Termez.

Other regions such as Qarshi, Samarkand, and Urgench exhibit average solar radiation, indicating a moderate potential for solar energy production.

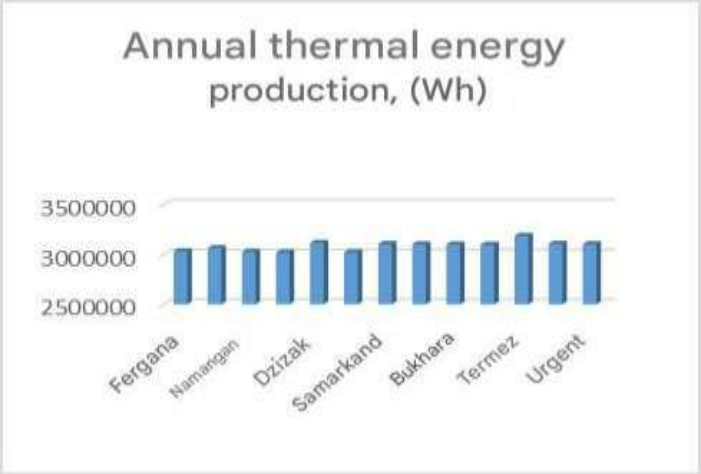

Figure 2 shows the amount of energy produced annually in various parts of Uzbekistan, expressed in units of heat energy—watt-hours (Wh)

The highest annual energy production is observed in the Qarshi and Termez regions, which is considerably higher than in other regions. This suggests that energy production capacities in Qarshi are more efficient or that natural conditions for energy production are more favorable there.

Uzbekistan's solar heating potential creates favorable conditions for introducing low-cost solar water heaters at the household level [18]. Nevertheless, public interest in domestic solar heating systems is very low, mainly due to high initial costs and the lack of locally adapted optimal designs. Therefore, there is a significant scientific and practical need in Uzbekistan to develop economically viable and technically simple solar water heating systems for local use.

Currently, national policy places great emphasis on developing the fuel–energy sector and addressing environmental problems associated with several important national economic challenges. Meeting these urgent tasks requires expanding the share of renewable energy sources. In many cases, the rational integration of solar energy with other energy sources helps to significantly conserve fuel and energy resources [19].

Solar water heaters operate by converting solar radiation into useful thermal energy through collection, storage and delivery. The performance of these systems depends on climate change, consumption and system design [20]. The analysis can be performed in three ways: (1) by heat transfer type (passive and active), (2) by collector technology (type) (flat-plate, vacuum-tube, concentrating), (3) by heat transfer medium (liquid, air, nanofluid) (see Fig. 3). At the same time, the application area (domestic and industrial/process and hybrid PV/T and SAHP) was also analyzed. Other engineering design aspects such as control, freeze/overheat protection, water quality management and compliance with standards can also affect durability and cost.

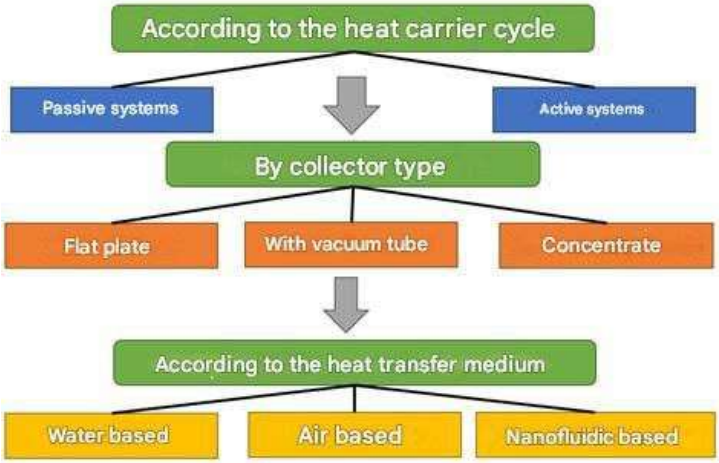

Figure 3. Classification of solar water heating systems

Passive systems do not use pumps or controllers; instead they rely on natural convective flow arising from thermosiphon or integral-storage designs. An integral-storage system is a form in which the collector and the heat-storage tank of the solar water heater are designed as a single unit combined within an insulated enclosure; this reduces the system's complexity and cost, but leads to energy losses during periods without sunshine and in winter; therefore it is suitable only for warm climates (Fig.4) [21].

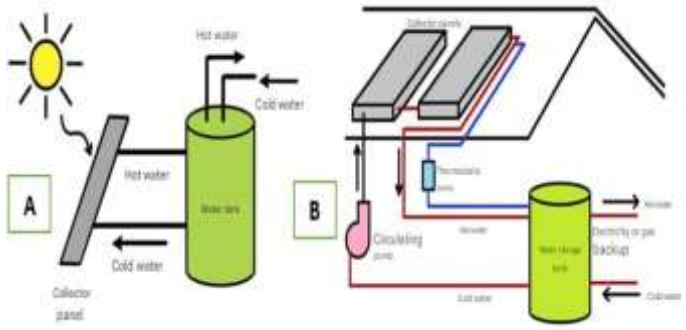

Figure 4. Classification of passive (a) and active (b) solar water heating systems.

Active systems use circulation pumps, differential thermostats and sometimes variable-speed control devices to modulate flow and reduce stratification of the collector outlet temperature (Fig. 4(b)). Direct (open-loop) designs circulate potable water through the collector [22], which maximizes heat-transfer efficiency but requires protection against corrosion and freezing. Indirect (closed-loop) systems transfer heat via a heat-transfer fluid (for example, a propylene glycol/water mixture) through a heat exchanger; this provides robust freeze protection and resistance to hard water at the cost of increased system balance complexity and pressure-drop losses in the exchanger [23].

A schematic of a simple flat-plate solar collector is shown in Fig.4(a). Solar radiation passes through the transparent cover and strikes a black, high-absorbance absorber plate; most of the energy is absorbed by the plate and then transferred to the heat-transfer fluid in the tubing, which carries the heat away for storage or use.

The underside of the absorber plate and the side walls of the casing are well insulated to reduce conductive heat losses. The fluid tubes can be welded to the absorber plate or manufactured as an integral part of the plate. The fluid tubes connect at both ends to larger diameter collector inlet and outlet pipes (supply and return).

A transparent cover (glazing) is used to reduce convective heat losses from the absorber plate; it limits heat transfer by creating a stagnant air layer between the plate and the glazing. It

also reduces the collector's radiative heat losses, because the glazing transmits short-wave solar radiation but is nearly opaque to the long-wave thermal radiation emitted by the absorber plate—this process is known as the "greenhouse effect".

Flat-plate collectors typically operate in a stationary mode and do not require a solar tracking (tracking) system. Collectors should be oriented toward the geographic equator: southward in the northern hemisphere and northward in the southern hemisphere. The optimal tilt angle of the collector equals the geographic latitude of the location, although this angle may be increased or decreased by about 10–15° depending on the application [24].

There are several ways to increase the efficiency of modern solar water heaters. By increasing the heat-transferring surfaces in the working chamber of solar water heaters and by using water pipes of various geometric shapes, the operating efficiency of the collectors can be increased to a certain extent. In many cases, a flat, solar-absorbing surface is used for the collectors. In such collectors, the heated water flow is laminar. Depending on the intensity of water heating through the absorber, the structure of the water heater can be divided into several types. The most common liquid flat-plate collector consists of a heat-absorbing panel (absorber) and channels (tubes) attached to it for the circulation of the heat transfer fluid. The upper part of the solar radiation-absorbing absorber has transparent insulation. All parts of this construction are attached to the casing, and the back and side surfaces are covered with a thermal insulation material.

The efficiency of solar water heaters largely depends on the shape and dimensions of the heat-absorbing surface (the absorber). Unlike conventional flat absorbers, conical absorbers increase hot-water production by directing the incoming solar radiation toward the center and accelerating convective flows [25]. Such shapes ensure a more uniform distribution of solar irradiance over the surface, leading to an increased absorption coefficient. Because the cone narrows upward, it also helps to economize and direct convective flows [26].

For conical solar water heaters, the absorber surface should receive maximal illumination. To achieve this, the geometric parameters (bottom radius R, top radius r, height h, and angle α) must be chosen optimally. The influence of each parameter on efficiency is evaluated using mathematical modeling, plots, analysis, and experimental observations.

2. Materials and Methods

The chapter extensively details the optimization methodology for the primary geometric dimensions of a truncated conical solar water heater, as well as their impact on solar irradiation exposure, heat exchange, and energy efficiency. As a result, efficient geometric shapes, materials, and the layout scheme for spiral pipes within the device are determined [27].

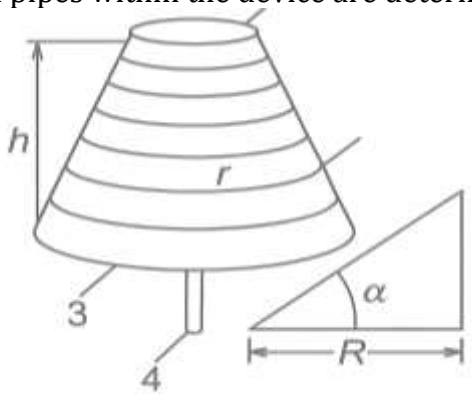

Figure 5. Schematic of a truncated conical solar water heater.

One of the most critical factors determining the efficiency of the truncated conical absorber, which serves as the structural form of the solar water heater, is its geometric parameters. Truncated cone-shaped collectors allow for directing solar radiation toward the

center, increasing the absorption surface area, and enhancing convective motion. In devices with such a shape, heat flows rise upward, leading to the faster formation of hot water.

The calculation of the primary geometric indicators of the truncated cone, including the lateral surface length (l), surface area (S), and volume (V), is of significant importance. In this regard, the following parameters are assumed: major radius R = 0.5 m, minor radius r = 0.2 m, and height h = 0.245 m.

Thus, the total heat absorption surface area of the truncated conical solar water heater is approximately S ≈0.94 m^2, which corresponds to the optimal illuminated surface area determined experimentally. This volume is considered sufficient for establishing a one-time hot water reserve. Such a surface configuration facilitates the comprehensive absorption of solar radiation.

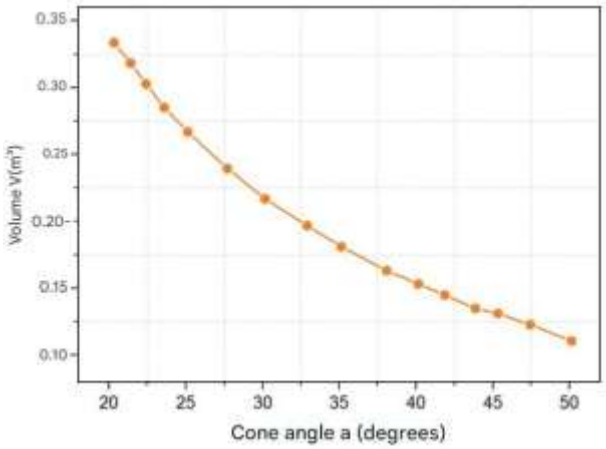

Figure 6. Effect of angle α on volume V.

As illustrated in the graph, the collector volume decreases as angle α increases. In the design process, it is crucial to achieve an optimal balance between height, volume, and the illumination angle. From a practical standpoint, $\alpha \approx 35^0$ is the most optimal solution for the collector, as it integrates volume, height, thermal efficiency, and structural feasibility. Due to the helical (spiral) arrangement of the copper pipes, an additional surface area for heat exchange is generated. The length of each pipe along the cone is determined by:

$$L_{quvur} = n \times \sqrt{(2\pi r_n)^2 + p^2} \qquad (1)$$

where r_n is the radius of each spiral turn, p is the pitch (height per turn), and n is the number of spiral turns. In the optimal state, the number of turns maximizes heat transfer without obstructing the incidence of solar radiation. Experimental results have confirmed that a pipe diameter of D = 15 mm yields optimal results.

Thus, the total heat absorption surface area of the truncated conical solar water heater corresponds to the experimentally determined optimal illuminated surface area. This volume is sufficient for establishing a one-time hot water reserve. The specific configuration of the surface facilitates the comprehensive absorption of solar rays.

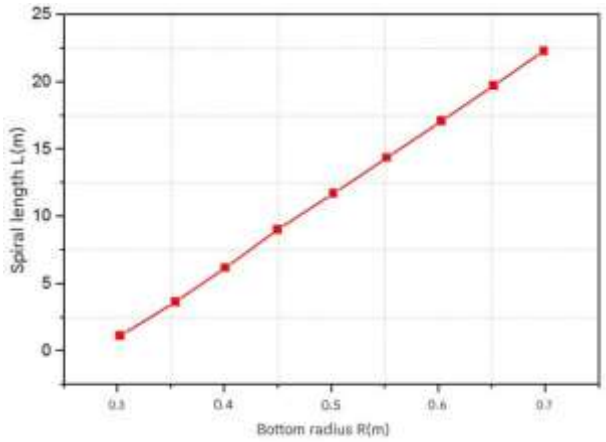

Figure 7. Relationship between the base radius R and the spiral pipe length L.

As illustrated in the graph, the total length of the spiral pipe L increases linearly as the turn radius rn increases. This graph is particularly significant for the arrangement of spiral copper pipes on the surface of a conical collector. When positioning the spiral copper pipes on the conical collector surface, it is necessary to optimize the turn radius rn by correlating it with the base radius R and the top radius r.

In the design of conical absorber collectors, the geometric angle of the cone—specifically, the angle α between its side wall and the vertical axis—directly determines the illumination of the collector surface and the efficiency of heat absorption. This angle is determined using the following formula:

$$\alpha = \arctan(R - r/h) \qquad (2)$$

Given the following collector dimensions: base radius R = 0.5 m, top radius r = 0.2 m, and height h = 0.245 m, the angle is calculated as follows:

For the solar collector to operate at maximum efficiency, the geometric angle of the cone (α) must be less than or equal to the maximum incidence angle of solar radiation on the Earth's surface:

$\alpha \leq \phi$

where ϕ is the solar incidence angle (dependent on geographic latitude and time of day). The condition $\phi \approx 35^{\circ}$ is the requirement for maximum efficiency, as solar rays strike the surface at a nearly perpendicular angle, the probability of shading is minimized, and the collector surface receives maximum illumination.

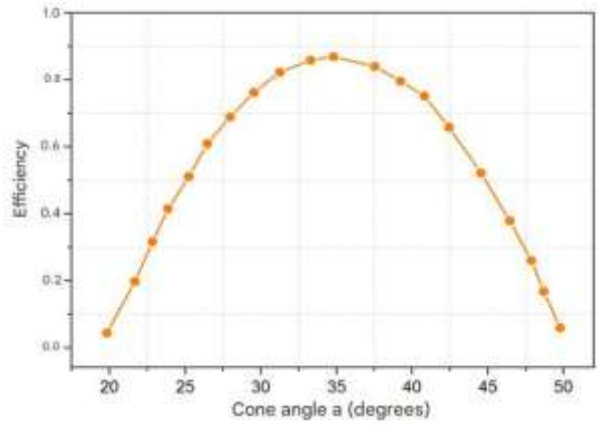

Figure 8. Effect of angle α on efficiency η.

The following idealized model illustrates the relationship between the angle and efficiency [28], where ηmax ≈0.85 is the maximum efficiency, αopt = 35^∘, and k = 0.0005 is an empirical coefficient.
Graphically, this forms a parabolic curve where η approaches its maximum at an angle of ϕ≈35^∘, and the efficiency gradually decreases as it deviates from this value.
If α≤30^∘, the collector becomes excessively elongated, and surface illumination decreases.
If α≥40^∘, the side of the surface opposite to the sun becomes shaded, leading to a drop in efficiency.
When arranging the spiral along the surface of a conical collector, the radius of each spiral turn (r_n) is determined either constantly or variably around the central axis of the cone [29]. This radius is defined by the following relationship:

$$r_n = r + \frac{(R-r)}{n} \times (i-1)$$

(3)

where: r_n_n is the radius of the spiral at the turn (m), i-is the turn sequence number $1 \leq i \leq n$, r and R are the top and bottom radii of the cone (m), respectively, and n is the total number of turns.

The length of each turn was determined as follows:

$$L_i = \sqrt{(2\pi r_n)^2} + p^2$$

(4)

where p is the turn height (pitch). The total length is:

$$L_{quvur} = \sum_{i=1}^{n} \sqrt{(2\pi r_n)^2} + p^2$$

(5)

This requirement ensures that the pipe structurally conforms to the conical shape and does not interfere with the externally illuminated surface. The outermost turn of the spiral pipe must not extend beyond the bottom radius of the collector. That is, the geometric condition $r_n \leq R$ must be satisfied. This ensures the structural integrity of the pipe's fit to the conical shape and prevents collision with the illuminated surface.

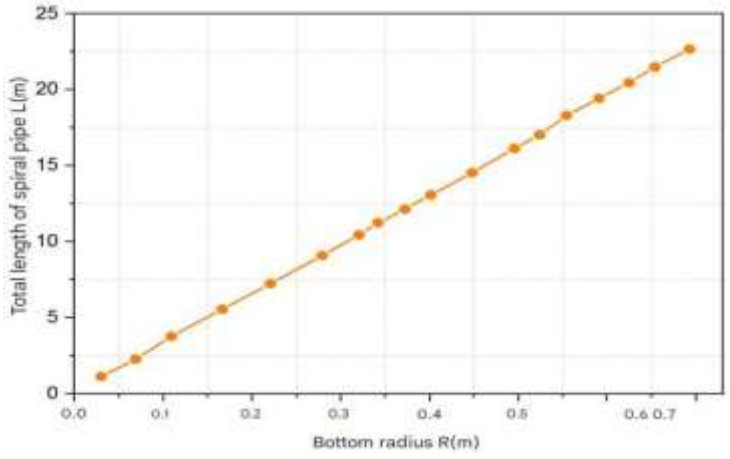

Figure 9. Dependence of the spiral pipe length on R (bottom radius).

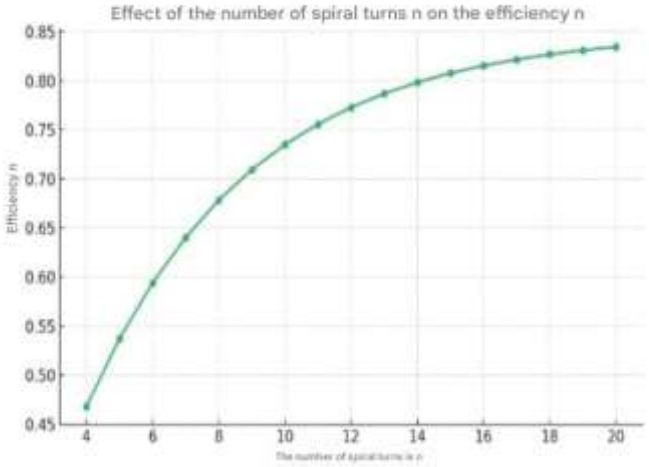

Figure 10. Influence of the number of spiral turns n on the spiral pipe length.

As shown in Fig. 9 the spiral pipe length increases almost linearly as the number of turns n increases. This indicates that material consumption increases as the spiral density rises [30].

Geometric optimization demonstrates that for a conical absorber, parameters of alpha = 35^0, h = 0.428 m, R = 0.5 m, and r = 0.2 m increase efficiency up to a maximum of 85%. The spiral copper pipes and deflector turns enhance heat exchange. This approach is fully synchronized in terms of thermal conductivity, water circulation, and solar illumination geometry, representing an optimal solution for energy efficiency and hot water production.

Convective Heat Exchange in Truncated Conical Solar Water Heaters

There are factors influencing the intensification of heat exchange processes in collectors. One of the primary methods involves installing special spiral pipes on the absorber surface of the truncated conical solar water heater collector. Solar water heater collectors typically exhibit low heat transfer characteristics due to the low thermal conductivity of water passing over flat surfaces. The main challenge in using water as a heat carrier is its low heat capacity and thermal conductivity, as well as the low heat transfer coefficient between the absorber and the water. The primary objective when using water as a heat carrier is to increase the heat transfer coefficient. Therefore, by employing appropriate methods to enhance thermal conductivity, the thermal efficiency of solar water heater collectors is improved. Compared to other types of volumetric solar water collectors, the heat transfer efficiency of this specific type is observed to be approximately 18–25% higher [31].

The objective defined on the theoretical basis of convective heat transfer is to determine the quantity of heat passing through an absorber surface that is being swept (washed) by a fluid flow. It must be particularly emphasized that heat flux always moves in the direction of a decreasing temperature gradient.

Newton's law of cooling can be utilized to calculate the heat transfer during the heat exchange process:

$$Q = \alpha F(t_c - t_{dev}) \quad (6)$$

Specifically, the heat flux transferred from the fluid to the wall or from the wall to the fluid is proportional to the surface area F participating in the heat exchange and the temperature gradient ΔT. Here, T_f is the temperature of the medium washing the wall surface. The proportionality coefficient α, which accounts for the specific conditions of heat exchange between the fluid and the surface of the solid body, is called the heat transfer coefficient.

Description of Water Flow over Cylindrical Surfaces and Variations in Heat Transfer.

A boundary layer forms on the surface of the opposite (rear) side of the solar water heater collector tubes, and two symmetric vortices appear behind the tube. The location of the boundary layer separation point depends on the Reynolds number (Re). When the Re number

is relatively low and the turbulence level of the incoming water flow is small, boundary layer separation is observed at an angle of 82–84° [32]. For the case of transverse water flow over a tube, the average heat transfer is calculated using the following formula:

$Nu=(0,43+CRe^{m}Pr^{0,38})\ \varepsilon$

(7)

The characteristic temperature is defined as the temperature of the incoming water, and the characteristic dimension is the diameter of the cylinder. The correction factor epsilon accounts for the turbulence level of the incoming flow (ε =1,0÷1,6). The coefficient C and the exponent m take the following values depending on the Re number:

$Re=1\div4\cdot10^{3}$, C=0,35, m=0,5;

$Re=4\cdot10^{3}\div4\cdot10^{4}$, C=0,20, m=0,62;

$Re=4\cdot10^{4}\div4\cdot10^{5}$, C=0,027, m=0,80. (8)

If the flow strikes the cylinder at an angle $\psi<90°$ irc, the heat transfer coefficient α calculated by equation (2.38) must be multiplied by α, $\varepsilon_{\varphi}\approx1-0,54\cos^{2}\psi$. If there is not a single tube but a whole bundle of tubes in the transverse flow, the heat exchange process becomes even more complex. In this case, heat transfer depends on the arrangement of the tubes in the bundle and the row number. Figure 2.2 illustrates the characteristics of fluid motion when the tubes are arranged horizontally.

The first row of tubes in the bundle is swept by an undisturbed fluid flow; therefore, alpha is lowest in this row. In subsequent rows, heat transfer proceeds much more intensely, and for the third and following rows, alpha remains almost identical. For tube bundles where $10^{3}<Re<10^{5}$ and $0,7<Pr<500$, heat transfer is determined from the following equation:

$$\overline{Nu}=C\,\mathrm{Re}^{m}\,P_{r}^{1/3}\left(\frac{\mathrm{Pr}_{c}}{\mathrm{Pr}_{g}}\right)^{1/3}\varepsilon_{S}\cdot\varepsilon_{i} \qquad (9)$$

For staggered (quincunx) arrangements, c = 0.41, m = 0.65; for in-line (aisle) arrangements, c = 0.26, m = 0.65. The correction factor ε_s accounts for the transverse S_1 and longitudinal S_2 pitch of the bundle. For parallel bundles, ε_s=1,12, $S_1/S_2\geq2$ when. The factor ε_I accounts for the reduction in heat transfer in the first and second rows of tubes. For the first row, ε_i=0,7 (staggered bundle) and ε_i=0,9 (in-line bundle); for the third and subsequent rows, ε_i=1

The average value of the heat transfer coefficient for the entire tube bundle is determined by the following formula:

$$\overline{\alpha}=\frac{\sum_{i=1}^{Z}\overline{\alpha_{i}}F_{i}}{\sum_{i=1}^{Z}F_{i}} \qquad (10)$$

where $\overline{\alpha}_i$ – i is the average heat transfer coefficient of the i-th row, F_i – i is the surface area of the th row, and Z is the total number of tubes in the bundle [33]. In solar water heater collectors, the water flow sweeps the absorber and the inner parts of the tubes, increasing heat exchange efficiency. If we consider the change in the heat transfer coefficient alpha relative to the surface temperature and water flow rate, the distribution of heat in the collector over time (Fig.11) is as follows:

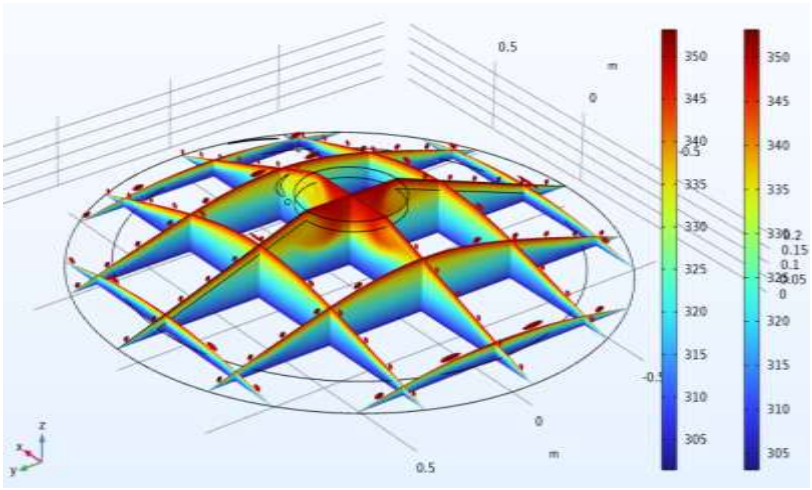

Figure 11. Variation of heat distribution in the working chamber of a solar water heater with a standard reservoir, reflector, and tube system at different times. a) Stage 1 of heat distribution; b) Stage 2 of heat distribution; c) Stage 3 of heat distribution.

t has been determined that the heat transfer capacity of the investigated solar water heater collector increases as a result of the intensification of heat exchange processes using a conical tube absorber, and the value of the heat transfer coefficient alpha is found to be 83.2 W/m^2°CThe third chapter of the dissertation focuses on heat distribution, which is a key indicator of the solar water heater collector's heat transfer performance, and a mathematical model has been developed .

Currently, solar water heater collectors are available in simple, complex, and storage-type structures. Simple solar water heater types include flat-plate collectors, while complex solar water heater types include vacuum and concentrating collectors. Storage-type solar water heaters consist of collectors where water accumulates in the absorber for a certain period and is heated by solar radiation.The developed solar water heater of this type also operates on the principle of the device model mentioned above. The dimensions of the conical channel solar water heater model are as follows: length - 427mm, large radius - 1000mm, small radius - 200mm, height - 245mm. Copper pipes for additional water heating are installed in the working chamber of this solar water heater.

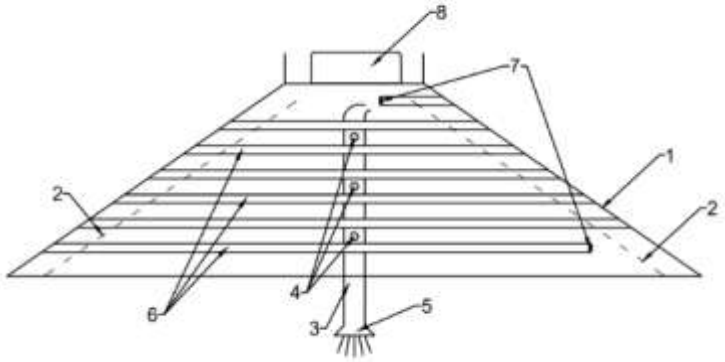

Figure 12. Principle Diagram of the Conical Channel Solar Water Heater
1-Blackened Metal Surface (Absorber), 2-Deflector, 3- Water Outlet Channel, 4- Auxiliary Rubber Hose for Hot Water Outlet, 5-Valve, 6- Water Channels, 7- Auxiliary Channel,8- Cover

Modeling

The heat distribution in the working chamber of a conical solar water heater collector is considered a very complex physical process. This is because multiple differential equations are solved simultaneously. The heat transfer equations for solid surfaces and fluids, along with the

Navier-Stokes equations for the motion of fluids or gases, are calculated together.

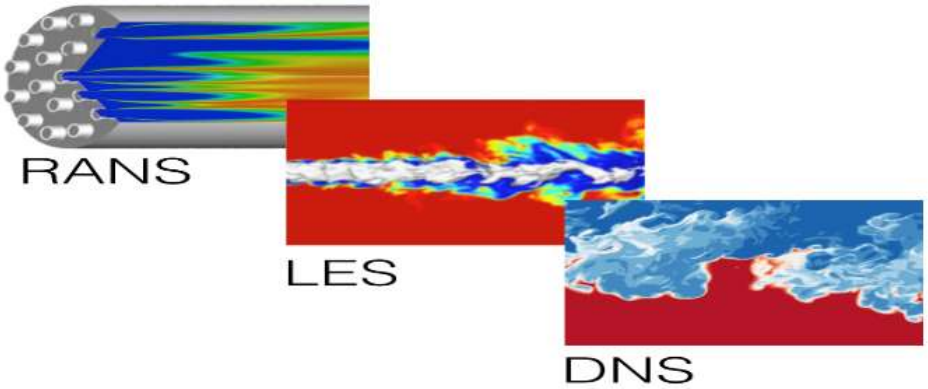

Figure 13. Approaches to Modeling Heat Transfer

The heat transfer equation in solid bodies is written as follows:

$$\rho C_p \frac{\partial T}{\partial \tau} = \frac{\partial}{\partial x}\left(k\frac{\partial T}{\partial x}\right) + \frac{\partial}{\partial y}\left(k\frac{\partial T}{\partial y}\right) + \frac{\partial}{\partial z}\left(k\frac{\partial T}{\partial z}\right) + Q + Q_{ted}; \quad (1)$$

Here, is *k*- thermal conductivity, C_p – is the specific heat capacity at constant pressure, *q* is the internal heat flux, and *Q* is the quantity of heat. This equation is used to determine heat transfer in solid surfaces that are in contact with each other [34].

To determine the solar radiation falling on the earth, the following equation is used:

$$\begin{aligned} J_i &= \varepsilon_i e_b(T) FEP_i(T) + \rho_{d,j} G_i \\ G_i &= G_{m,i} + G_{amb,j} + G_{ext,j} \\ G_{amb,i} &= F_{amb,j}\varepsilon_{amb} e_b(T_{amb}) FEP_i(T_{amb}) \\ e_b(T) &= n^2\sigma T^4,\ FEP_i(T) = \frac{15}{\pi^4}\int_{C_2/(\lambda_i - l^T)}^{C_2/(\lambda_i T)} \frac{x^3}{1-e^x}dx \end{aligned} \quad (2)$$

Here, *FEP* is the fractional emissive power, T_{amb} is the ambient temperature, ε – is the radiation coefficient, G_{amb} – is the ambient radiation, G_m – is the mutual surface radiation, G_{ext} – is the external radiation, F_{amb} – is the view factor of the ambient environment, e_b – is the radiation power, and ε_i – is the emissivity of the fraction.

To determine the motion of liquids or gases, the Navier-Stokes differential equations are used.

$$\begin{cases} \frac{\partial \rho}{\partial \tau} + \frac{\partial \rho V_x}{\partial x} + \frac{\partial \rho V_y}{\partial y} + \frac{\partial \rho V_z}{\partial z} = 0. \\ \rho\frac{\partial V_x}{\partial \tau} + \rho V_x\frac{\partial V_x}{\partial x} + \rho V_y\frac{\partial V_x}{\partial y} + \rho V_z\frac{\partial V_x}{\partial z} + \frac{\partial p}{\partial x} = \\ = \frac{\partial}{\partial x}\left(\nu\rho\frac{\partial V_x}{\partial x}\right) + \frac{\partial}{\partial y}\left(\nu\rho\frac{\partial V_y}{\partial y}\right) + \frac{\partial}{\partial z}\left(\nu\rho\frac{\partial V_z}{\partial z}\right); \\ \rho\frac{\partial V_y}{\partial \tau} + \rho V_x\frac{\partial V_y}{\partial x} + \rho V_y\frac{\partial V_y}{\partial y} + \rho V_z\frac{\partial V_y}{\partial z} + \frac{\partial p}{\partial y} = \\ = \frac{\partial}{\partial x}\left(\nu\rho\frac{\partial V_y}{\partial x}\right) + \frac{\partial}{\partial y}\left(\nu\rho\frac{\partial V_y}{\partial y}\right) + \frac{\partial}{\partial z}\left(\nu\rho\frac{\partial V_y}{\partial z}\right); \\ \rho\frac{\partial V_z}{\partial \tau} + \rho V_x\frac{\partial V_z}{\partial x} + \rho V_y\frac{\partial V_z}{\partial y} + \rho V_z\frac{\partial V_z}{\partial z} + \frac{\partial p}{\partial z} = \\ = \frac{\partial}{\partial x}\left(\nu\rho\frac{\partial V_z}{\partial x}\right) + \frac{\partial}{\partial y}\left(\nu\rho\frac{\partial V_z}{\partial y}\right) + \frac{\partial}{\partial z}\left(\nu\rho\frac{\partial V_z}{\partial z}\right) - F_z; \end{cases} \quad (11)$$

Here, V_x, V_y, V_z are the velocity components of the flow, ρ-is the density, F_z-is the gravitational force, ν - is the kinematic viscosity of the fluid, and *p*- is the pressure. This equation is used to determine the velocities and pressure of the fluid flow.

The heat transfer equation in fluids is written as follows:

$$\begin{cases} \rho C_p \frac{\partial T_2}{\partial \tau} + \rho C_p V_x \frac{\partial T_2}{\partial x} + \rho C_p V_y \frac{\partial T_2}{\partial y} + \rho C_p V_z \frac{\partial T_2}{\partial z} = \\ = \frac{\partial}{\partial x}\left(k \frac{\partial T_2}{\partial x}\right) + \frac{\partial}{\partial y}\left(k \frac{\partial T_2}{\partial y}\right) + \frac{\partial}{\partial z}\left(k \frac{\partial T_2}{\partial z}\right) + Q + Q_p + Q_{vd}; \end{cases} \quad (12)$$

Equation 4 is similar to Equation 1, with the main difference being that it includes a convective term that accounts for the velocity in fluid flow.

The heat transfer coefficient obtained from convective heat exchange is:

$$h = \frac{k}{D_h} Nu \quad (13)$$

Where *k*-is the thermal conductivity coefficient of the heat carrier fluid; *Nu*-is the Nusselt number; and D_h-is the equivalent diameter, which is determined as follows:

$$D_h = \frac{4Wd}{2(W+d)} \quad (14)$$

Where d is the equivalent diameter of the channel (m).

$\mathrm{Re} < 340$

$$Nu = 5.4 + \frac{0.00190\left[\mathrm{Re}\,\mathrm{Pr}\left(\frac{D_h}{L}\right)\right]^{1.71}}{1 + 0.0053\left[\mathrm{Re}\,\mathrm{Pr}\left(\frac{D_h}{L}\right)\right]^{1.71}} \quad (15)$$

Where *Re* is the Reynolds number; *Pr* is the Prandtl number; and *L* is the channel length, and $340 \le \mathrm{Re} \le 3400$

$$Nu = 0.116\left(\mathrm{Re}^{2/3} - 125\right)\mathrm{Pr}^{1/3}\left[1 + \left(\frac{D_h}{L}\right)^{2/3}\right]\left(\frac{\mu}{\mu_w}\right) \quad (16)$$

Where $\mu -$ is the dynamic viscosity of the heat carrier fluid at temperature $T_f -$ and is the dynamic viscosity of the heat carrier fluid at temperature T_0.

Discretization of Navier–Stokes and Heat Distribution Equations and Solving Based on COMSOL Multiphysics [35].

The governing physical equations in modeling the processes of heat exchange and fluid motion within a conical solar water heater collector are the Navier–Stokes equations and the heat distribution equation. These equations are discretized and solved using the Finite Element Method (FEM) within the COMSOL Multiphysics environment. The mathematical form of these equations, the numerical scheme, and the iterative solution configurations in COMSOL are detailed below.

$$\rho C_p\left(\frac{\partial T}{\partial \tau} + \overline{U} \cdot \nabla T\right) = \nabla \cdot (k \nabla T) + Q_{um}. \quad (16)$$

This equation represents the temperature change due to heat capacity, flow, and diffusion.

Discretized representation (2D, Central difference + time derivative):

$$\rho C_p\left(\frac{T_{i,j,k}^{n+1} - T_{i,j,k}^{n}}{\Delta\tau} + V_{x,i,j,k} \cdot \frac{T_{i+1,j,k}^{n+1} - T_{i-1,j,k}^{n}}{2\Delta x} + V_{y,i,j,k} \cdot \frac{T_{i,j+1,k}^{n+1} - T_{i,j-1,k}^{n}}{2\Delta y} + V_{z,i,j,k} \cdot \frac{T_{i,j,k+1}^{n+1} - T_{i,j,k-1}^{n}}{2\Delta z}\right) =$$

$$= k\left(\frac{T_{i+1,j,k}^{n+1} - 2T_{i,j,k}^{n} + T_{i-1,j,k}^{n}}{\Delta x^2} + \frac{T_{i,j+1,k}^{n+1} - 2T_{i,j,k}^{n} + T_{i,j-1,k}^{n}}{\Delta y^2} + \frac{T_{i,j,k+1}^{n+1} - 2T_{i,j,k}^{n} + T_{i,j,k-1}^{n}}{\Delta z^2}\right) + Q_{um}.$$

This equation is solved by COMSOL based on the central difference scheme.

The system of 3 equations can be expressed in matrix form as follows:

$$\frac{\partial \Phi}{\partial t}+V_x\frac{\partial \Phi}{\partial x}+V_y\frac{\partial \Phi}{\partial y}+V_z\frac{\partial \Phi}{\partial z}=\frac{\partial}{\partial x}\left(\mathrm{A}\frac{\partial \Phi}{\partial x}\right)+\frac{\partial}{\partial y}\left(\mathrm{B}\frac{\partial \Phi}{\partial y}\right)+\frac{\partial}{\partial z}\left(C\frac{\partial \Phi}{\partial z}\right)+\Pi^{\Phi}.$$

$$\Phi=\begin{pmatrix}V_x\\V_y\\V_z\end{pmatrix},\mathrm{A}=\begin{pmatrix}(\nu)\rho\\(\nu)\rho\\(\nu)\rho\end{pmatrix},B=\begin{pmatrix}(\nu)\rho\\(\nu)\rho\\(\nu)\rho\end{pmatrix},C=\begin{pmatrix}(\nu)\rho\\(\nu)\rho\\(\nu)\rho\end{pmatrix},\Pi^{\Phi}=\begin{pmatrix}0\\0\\g\end{pmatrix}.$$

When solving convective terms, the countercurrent scheme uses the quadratic interpolation method. This method is used to solve convective (advection) equations more accurately and is calculated using the following formula:

When calculating diffusion (viscosity) terms, the central difference scheme is used. This scheme is widely used to simplify diffusion processes and is based on the following formula:

$$\frac{\Phi^{n+1}_{i,j,k}-\Phi^{n}_{i,j,k}}{\Delta t}+\frac{\left(F_e+|F_e|\right)\Phi^{n}_{i+1,j,k}+\left(|F_e|+|F_w|+F_e-F_w\right)\Phi^{n}_{i,j,k}-\left(F_w+|F_w|\right)\Phi^{n}_{i-1,j,k}}{2\Delta x}+$$

$$+\frac{\Phi^{n}_{i,j+1,k}\left(F_n-|F_n|\right)+\Phi^{n}_{i,j,k}\left(\left(|F_n|+F_n\right)+\left(|F_s|-F_s\right)\right)-\Phi^{n}_{i,j-1,k}\left(|F_s|+F_s\right)}{2\Delta y}+$$

$$+\frac{\Phi^{n}_{i,j,k+1}\left(F_u-|F_u|\right)+\Phi^{n}_{i,j,k}\left(\left(|F_u|+F_u\right)+\left(|F_d|-F_d\right)\right)-\Phi^{n}_{i,j,k-1}\left(|F_d|+F_d\right)}{2\Delta z}=$$

$$=\left(A\frac{\Phi^{n}_{i+1,j,k}-2\Phi^{n}_{i,j,k}+\Phi^{n}_{i-1,j,k}}{\Delta x}+B\frac{\Phi^{n}_{i,j+1,k}-2\Phi^{n}_{i,j,k}+\Phi^{n}_{i,j-1,k}}{\Delta y}+C\frac{\Phi^{n}_{i,j,k+1}-2\Phi^{n}_{i,j,k}+\Phi^{n}_{i,j,k-1}}{\Delta y}\right)-\Pi^{\Phi}$$

$$F_e=\frac{\left(\Phi^{n}_{i+1,j,k}+\Phi^{n}_{i,j,k}\right)}{2},\quad F_w=\frac{\left(\Phi^{n}_{i,j,k}+\Phi^{n}_{i-1,j,k}\right)}{2},F_n=\frac{\left(\Phi^{n}_{i,j+1,k}+\Phi^{n}_{i,j,k}\right)}{2},$$

$$F_s=\frac{\left(\Phi^{n}_{i,j,k}+\Phi^{n}_{i,j-1,k}\right)}{2},F_u=\frac{\left(\Phi^{n}_{i,j,k+1}+\Phi^{n}_{i,j,k}\right)}{2},\quad F_d=\frac{\left(\Phi^{n}_{i,j,k}+\Phi^{n}_{i,j,k-1}\right)}{2}$$

General analysis of the results obtained by numerical modeling of the heat exchange processes of a conical solar water heater collector [36].

The results obtained include the heat exchange and heat dissipation, as well as the water movement velocities, including under different conditions with solar radiation of 250-910 W/m2. The numerical results were obtained for volumetric, reflector volumetric, and volumetric solar water heaters with a cylindrical tube and reflector, and the main thermal parameters were compared.

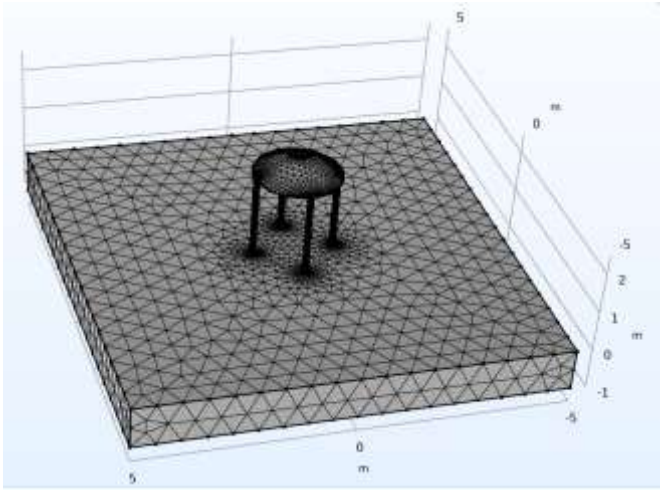

Figure 14. Conical volume water heater collector grids

The efficiency of solar water heating systems depends on the water flow velocity, the design of the working chamber, and heat exchange processes. In this study, the water velocity in the working chamber of a solar water heater with a simple reservoir varies within the range of 0.5–1.5 m/s, and the results obtained at different times are presented below.

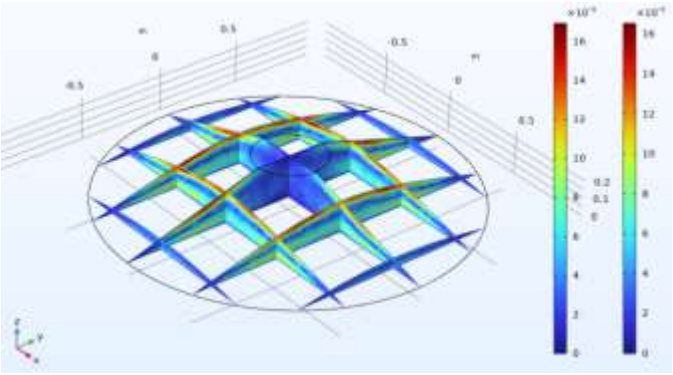

Figure 15. The variation of water velocity in the range of 0.5–1.5*10 $^{-2}$ m/s at different times within the working chamber of a solar water heater with a simple reservoir.

At a water flow velocity of 0.5*10 $^{-2}$ m/s, heat exchange occurs relatively slowly due to the low convective heat transfer rate. At this velocity, a more intense heat exchange process can be observed in the upper layers of the water, whereas heat distribution in the lower layers is found to be non-uniform.

The efficiency of solar-powered water heating systems depends on several factors, the most significant of which include the water flow velocity, the design of the working chamber, and heat exchange processes. To enhance the system's operational efficiency, a deflector is installed, which accelerates the convective heat exchange process.

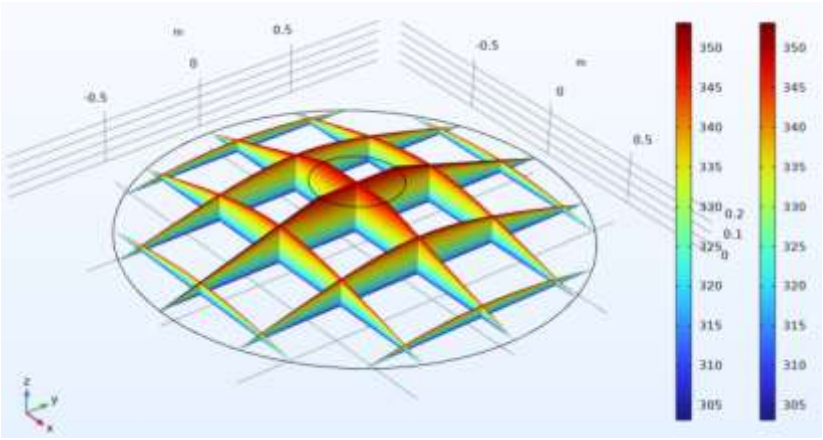

Figure 16. Heat distribution at different times in a solar water heater with a simple reservoir.

The maximum temperature is achieved when the water velocity is 1.0–1.5 m/s and solar radiation is 800–1000 W/m^2. This condition is considered optimal for increasing the overall efficiency of the water heater.

In a solar water heater with a simple reservoir, the velocity vectors change with variations in heat quantity over different times. The variation of velocity vectors in a solar water heater with a simple reservoir is a key indicator of heat exchange processes. Effective management of this process depends on the intensity of solar radiation, water temperature, and the thermotechnical characteristics of the reservoir.

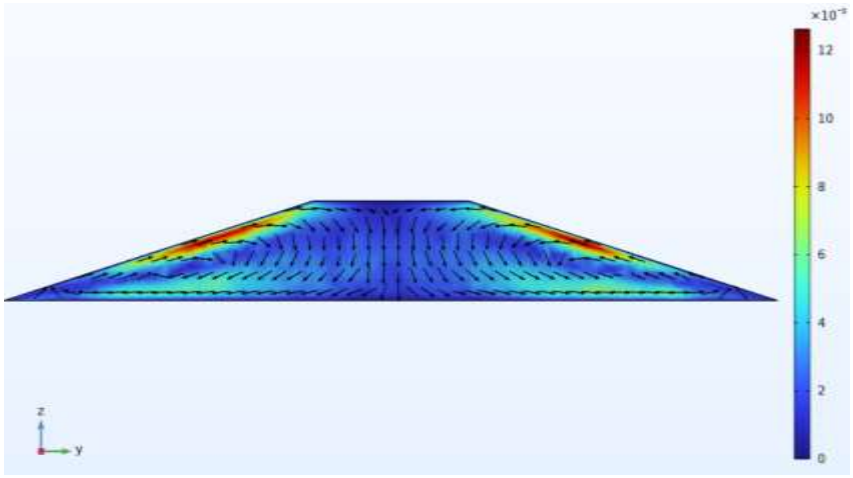

Figure 17. Variation of velocity vectors at different times in a solar water heater with a simple reservoir.

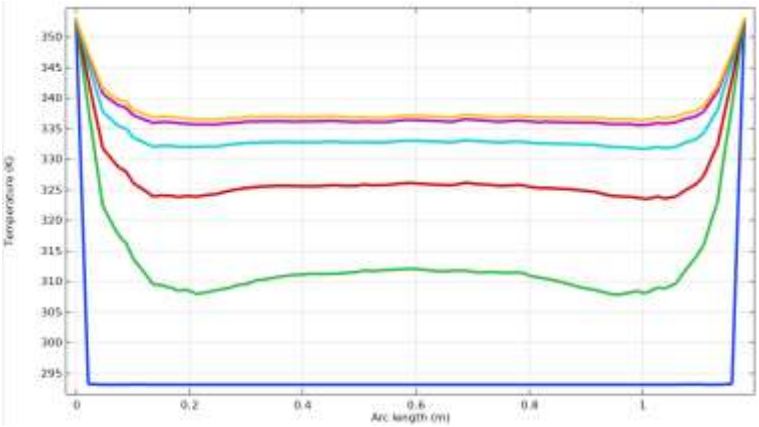

Figure 18. Variation of water temperature at different times in a solar water heater with a simple reservoir.

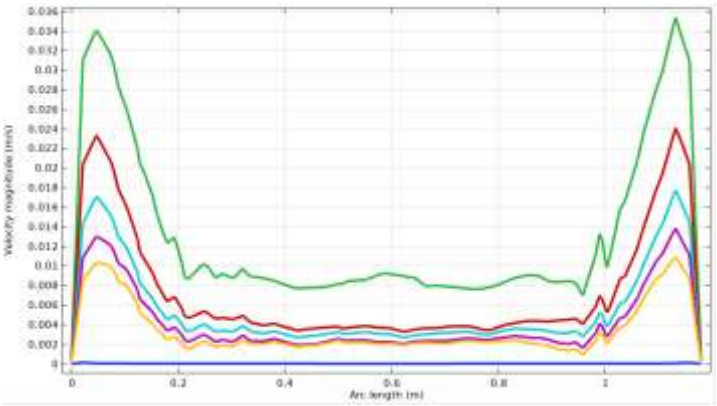

Figure 19. Variation of water velocity at different times in a solar water heater with a simple reservoir.

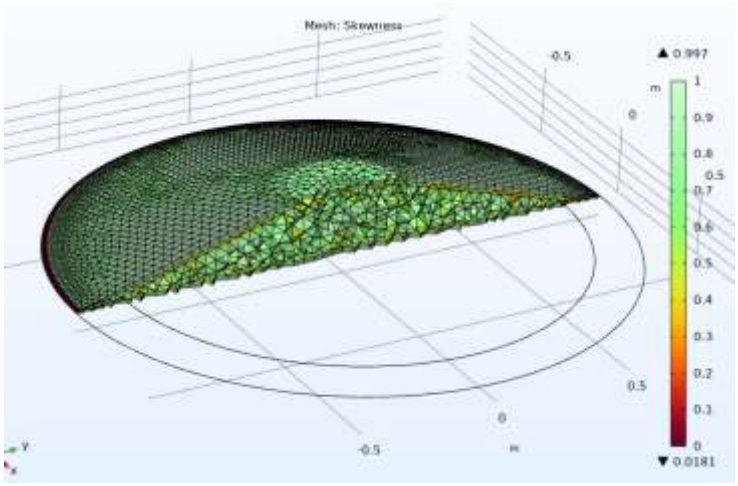

Figure 20. Discretization of a solar water heater with a simple reservoir and a reflector into small meshes (73,414 elements).

The efficiency of solar water heating systems depends on several factors, the most important of which are: water flow velocity, the design of the working chamber, and heat exchange processes. To increase the system's operational efficiency, a reflector is installed, which accelerates the convective heat exchange process.

The results obtained from this modeling analyze the variation of water velocity in the range of 0.5-1.5 m/s at different times within the working chamber of a simple reservoir solar water heater with a reflector. The results are presented below.

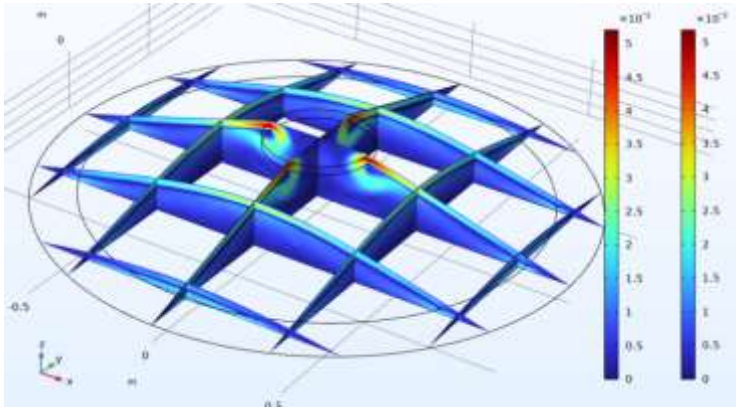

Figure 21. Variation of water velocity in the range of 0.5–1.5 m/s at different times within the working chamber of a solar water heater with a simple reservoir and a deflector.

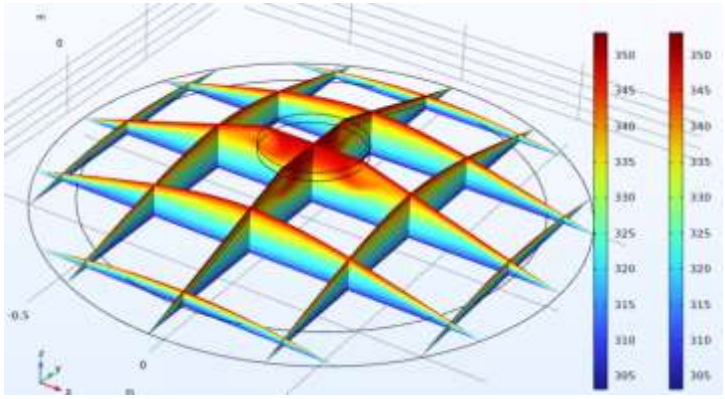

Figure 22. Variation of heat distribution at different times within the working chamber of a simple reservoir solar water heater with a reflector.

In solar water heaters with a simple reservoir and a reflector, when the water velocity is in the range of 1.0-1.5 m/s, the convective heat transfer coefficient significantly increases. In such conditions, the internal circulation of water allows for uniform heat distribution, which, in turn, increases the operating efficiency of the solar water heater device.

Depending on the intensity of solar radiation, the heat exchange process occurs in the working chamber of a simple reservoir solar water heater with a reflector. At different times, this process provides the following indicators regarding the distribution of water temperature[37].

In a simple reservoir solar water heater with a reflector, the velocity vectors change at different times in conjunction with variations in the heat quantity. This change in velocity vectors is one of the key indicators of heat exchange processes. Effective management of this process depends on the intensity of solar radiation, the water temperature, and the thermotechnical characteristics of the reservoir.

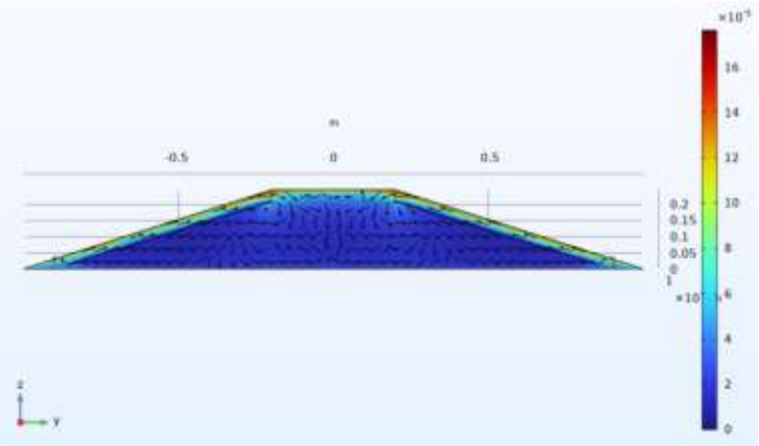

Figure 23. Variation of velocity vectors at different times in a simple reservoir solar water heater with a reflector.

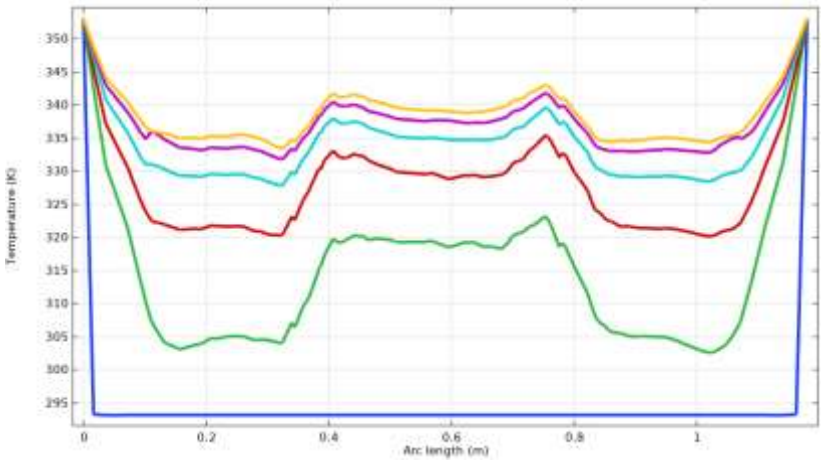

Figure 24. Variation of water temperature at different times in a simple reservoir solar water heater with a reflector.

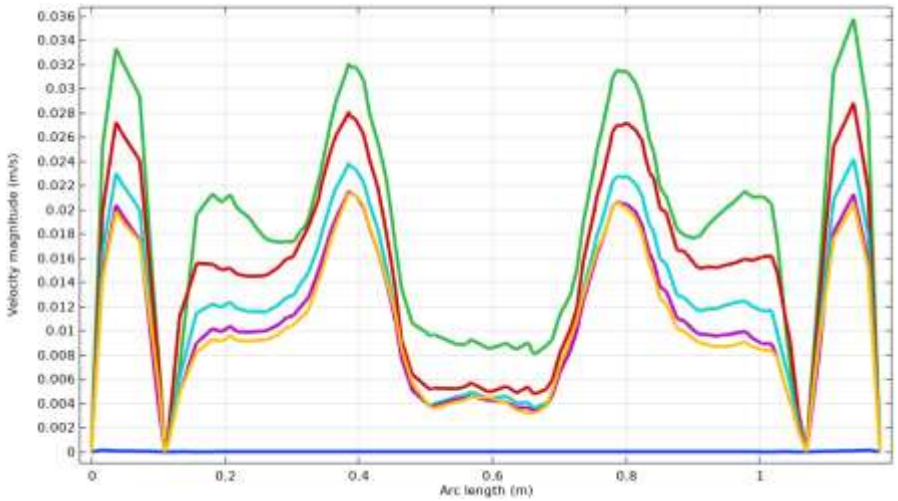

`Figure 25. Variation of water velocity at different times in a simple reservoir solar water heater with a simple reservoir.

In solar water heaters equipped with a simple reservoir and a deflector, the convective heat transfer coefficient increases significantly when the water velocity is within the 1.0–1.5 m/s range. Under these conditions, the internal circulatory motion of the water enables uniform heat distribution, which in turn enhances the operational efficiency of the solar water heating device.

The device helps increase energy efficiency and raise the water temperature in a short amount of time. This is especially important in areas where solar radiation intensity is low.

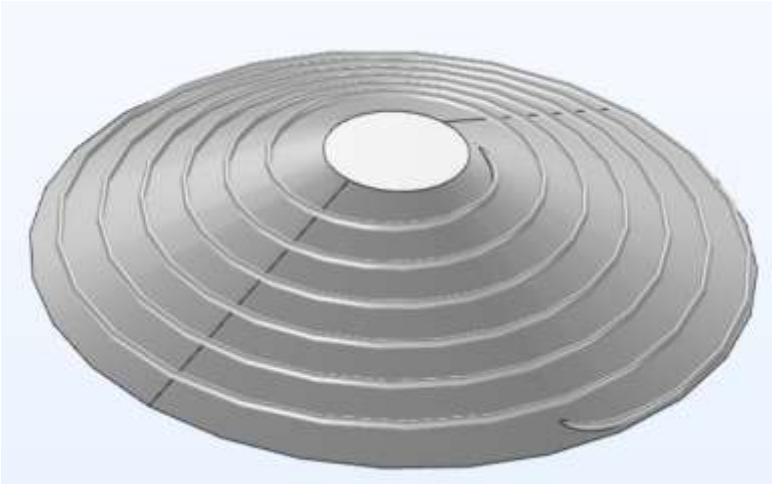

Figure 26. General View of the Working Volume of a Solar Water Heater with a Simple Reservoir, Deflector, and Pipe System

The efficiency of hot water systems using solar energy depends on a number of important factors, including the velocity of the water flow, the design of the working chamber, and heat exchange processes. In these systems, the water flow velocity and heat transfer processes in the working chamber play a crucial role in increasing efficiency. During the research, the effect of varying water flow velocities in the range of 0.5-1.5 m/s on efficiency at different times was studied in the working chamber of a solar water heater with a simple reservoir, deflector, and pipe system[38,39].

The pipe system, along with ensuring water flow, expands the heat transfer surface and ensures a uniform temperature distribution. It was noted that when the water flow velocity in the system was higher (in the range of 1.0-1.5 m/s), the convective heat transfer coefficient increased significantly. This improved the internal circulation of the water, helping to distribute the heat uniformly. At a lower velocity (0.5 m/s), the heat exchange occurred relatively slower,

and a decrease in efficiency was observed. Based on the results, improving the design of the working chamber and optimal placement of deflectors can help increase the overall efficiency of the system. The results observed at different times show the need to manage the heat exchange process in accordance with the water flow velocity. Thus, these systems can be further optimized to improve internal heat transfer and energy efficiency.

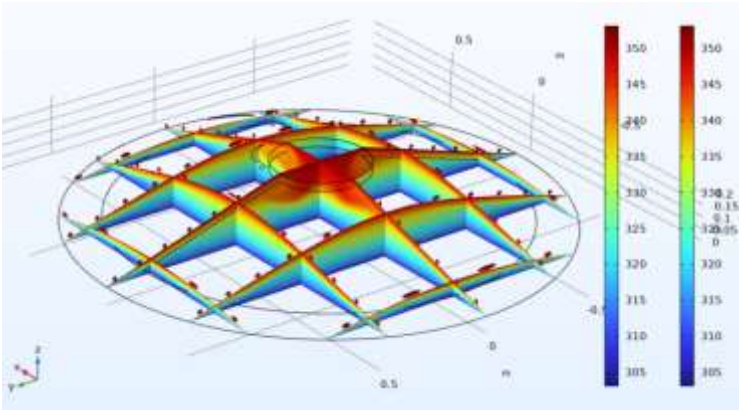

Figure 27. Variation in Heat Distribution at Different Times in the Working Chamber of a Solar Water Heater with a Simple Reservoir, Deflector, and Pipe System.

The proposed technology—comprising a solar water heater with a simple reservoir, a deflector, and a piping system—has been developed based on the optimization of existing systems, enabling a significant enhancement in energy efficiency. This system offers the following advantages:

Deflectors: Optimized for the efficient collection and redirection of solar energy into the working chamber, allowing for maximum utilization of solar radiation.

Piping System: Facilitates variable and turbulent water flow, ensuring that heat exchange occurs throughout the entire volume. Furthermore, due to the intensification of water movement and the heat transfer surface, the effective heat exchange area is expanded, leading to increased thermal efficiency.

With the improved device, heat output and efficiency parameters have been enhanced by 15–20%. This has a significant positive impact on the heating rate and operational stability of the solar water heater. The device increases energy efficiency and facilitates rapid water temperature elevation, which is particularly vital in regions with low solar radiation intensity [40].

3. Results and Discussion

In a solar water heater with a simple reservoir, deflector, and pipe system, the change in velocity vectors directly affects the water's heat exchange processes. Due to the variation in water flow velocity and the amount of heat at different times, the velocity vectors also change dynamically. These changes in velocity vectors are one of the main indicators of heat exchange processes. To effectively manage this process, the intensity of solar radiation, the temperature of the water, and the thermal-technical properties of the reservoir are important factors. By optimizing these factors, it is possible to achieve an increase in the overall efficiency of the system.

Based on the findings, optimizing the working chamber's configuration, along with the strategic placement of deflectors and the implementation of a piping system, facilitates an enhancement in the overall efficiency of the solar water heater. The observations recorded over various time intervals underscore the necessity of regulating the heat exchange process in accordance with the water flow velocity. Furthermore, the heat distribution in volumetric solar water heater collectors featuring three distinct geometric designs is presented.

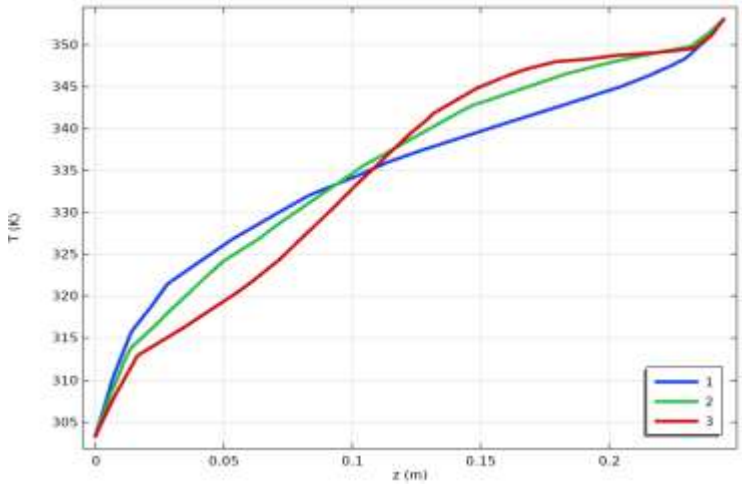

Figure 28. Temperature dependence of heat distribution in solar water heaters.

1-Simple volumetric solar water heater; 2-Volumetric solar water heater with a deflector; 3-Volumetric solar water heater collector with a deflector and a pipe system.

The volumetric solar water heaters investigated in this study are presented in three distinct structural configurations: 1) a simple volumetric solar water heater, 2) a volumetric solar water heater with a deflector, and 3) a volumetric solar water heater collector equipped with both a deflector and a pipe system. Among these systems, the device exhibiting the highest thermal efficiency is the Type 3 collector, which features the integrated deflector and pipe system.

4. Conclusion

In a simple volumetric solar water heater, solar radiation enters the working chamber only through direct exposure. While this device features a simple construction, its heat exchange surface is limited and the water flow is relatively slow, resulting in low thermal efficiency.

The heat exchange processes occurring in conical tubular solar water heater collectors, including convective heat exchange processes, were studied. Additionally, to determine the heat transfer capabilities of flat-surface absorbers and non-uniform (irregular) absorbers under convective conditions, the heat transfer coefficient (α) was identified within the range of 6–100 $W/(m^2 \cdot °C)$.

Based on experimental results conducted under specific conditions for a simple truncated conical solar water heater collector without a deflector, the heat transfer coefficient was calculated as $\alpha = 25.2\ W/(m^2 \cdot °C)$ with a Nusselt number Nu = 83.2. For truncated conical tubular absorber collectors with a deflector, the heat transfer coefficient was found to be 38.2 $W/(m^2 \cdot °C)$ with Nu = 126.1.

The characterization of the water flow washing across the circumference of the conical surfaces, the variation in heat transfer, and the dependence of these processes on the Reynolds number and boundary layer separation were analyzed. For tube bundles within the ranges of 10^3 < Re < 10^5 and 0.7 < Pr < 500, the Nusselt number Nu = 126.1, which characterizes the heat transfer capacity of the device, was determined using the heat transfer equation."

The volumetric solar water heater with a deflector utilizes a deflector to collect and direct solar radiation into the central working chamber. In this case, the heat transfer process is slightly intensified as the deflectors gather solar energy more actively. However, due to the irregular movement of water and incomplete heat distribution within the chamber, maximum efficiency is not achieved.

The volumetric solar water heater collector with deflectors and tubes combines all the advantages of the previous designs. Deflectors are used to capture a greater amount of solar radiation, while the tube system ensures the efficient distribution of water flow. In this system, internal convective movements are enhanced, the heat transfer surface is expanded, and the temperature is distributed uniformly. According to numerical modeling results, this specific device demonstrates 15–20% higher thermal efficiency and enables faster, more uniform heating of water.

The design of the third type—the volumetric solar water heater collector with deflectors and tubes—is considered the most optimal and represents the most effective solution for increasing energy efficiency in heat exchange systems.

References

[1] Y. N. Maksimova, "Saving renewable energy resources at the expense of using renewable energy sources," Scientific Progress, vol. 1, no. 6, p. 1266, 2021.

[2] A. N. Ortiqov, Sh. M. Yuldasheva, T. Sh. Karabaev, and R. D. Najmiddinov, Sanoat korxonalarida ishlab chiqarishni tashkil etish. Toshkent, O'zbekiston: Mehnat, 2004.

[3] A. D. Bayramov and L. Ushakova, Ispolzovanie solnechnoy energii. Ashgabat, Turkmenistan, 1973.

[4] Y. Y. Rafikova, "Geoinformatsionnoe kartografirovanie resursov vozobnovlyaemykh istochnikov energii," Ph.D. dissertation, Moscow, Russia, 2015.

[5] IRENA, Renewable Capacity Statistics 2024. Abu Dhabi, UAE: International Renewable Energy Agency, 2024.

[6] IEA, Global Hydrogen Review 2023. Paris, France: International Energy Agency, 2023.

[7] S. A. Kalogirou, Solar Energy Engineering: Processes and Systems, 2nd ed. Amsterdam, Netherlands: Elsevier, 2014.

[8] N. R. Esanaliyeva, S. F. Ergashev, and V. I. Ibrohimov, "Yer sharoitida quyosh energetik qurilmalaridan foydalanish usullari," NamDU Ilmiy Axborotnomasi, no. 4, pp. 42–45, 2022.

[9] K. Ukoba et al., "Adaptation of solar energy in the Global South," Heliyon, vol. 10, e28009, 2024.

[10] I. Yildiz, "Solar energy," in Comprehensive Energy Systems, 2018, pp. 638–668.

[11] A. B. Awan and Z. A. Khan, "Recent progress in renewable energy," Renewable and Sustainable Energy Reviews, vol. 33, pp. 236–253, 2014.

[12] J. A. Duffie and W. A. Beckman, Solar Engineering of Thermal Processes. Hoboken, NJ, USA: Wiley, 2013.

[13] M. I. A. Zaini et al., "Innovative water-cooling system for photovoltaic systems," Case Studies in Thermal Engineering, vol. 70, 2025.

[14] O. Hachchadi et al., "Techno-economic assessment of solar systems," Energy Conversion and Management, vol. 297, 2023.

[15] R. Shukla et al., "Recent advances in solar water heating systems," Renewable and Sustainable Energy Reviews, vol. 19, pp. 173–190, 2013.

[16] IRENA, Renewable Energy Statistics 2022. Abu Dhabi, UAE, 2022.

[17] UNDP, Tax Incentives for Renewable Energy. New York, NY, USA, 2022.

[18] M. M. A. Khan et al., "Evaluation of solar collector designs," Solar Energy, vol. 166, pp. 334–350, 2018.

[19] M. Koriev et al., "Alternative energy resources of Uzbekistan," Dera Natung Government College Research Journal, vol. 7, no. 1, pp. 20–31, 2022.

[20] N. R. Avezova et al., "Heating and cooling degree-days in Uzbekistan," IOP Conf. Ser.: Earth Environ. Sci., vol. 939, 2021.

[21] J. R. Zaynalov and S. S. Alieva, "Alternative energy development in Uzbekistan," E3S Web of Conferences, vol. 403, 2023.

[22] B. Isroilova et al., "Modernization of heating systems in Uzbekistan," E3S Web of Conferences,

vol. 574, 2024.
[23] G. Wang et al., “Multi-energy complementary power systems,” Renewable and Sustainable Energy Reviews, vol. 199, 2024.
[24] U. Jordan and K. Vajen, “Influence of DHW load profile,” Solar Energy, vol. 69, 2001.
[25] S. Kalogirou, “Solar industrial process heat applications,” Applied Energy, vol. 76, no. 4, pp. 337–361, 2003.
[26] J. F. Kreider, The Solar Heating Design Process. New York, NY, USA: McGraw-Hill, 1982.
[27] N. V. Khorchenko, Individual Solar Installations. Moscow, Russia, 1991.
[28] M. M. Mukhitdinov, S. F. Ergashev, and J. I. Isakulov, Quyosh energiyasidan foydalanish. Toshkent, O‘zbekiston, 1999.
[29] D. Y. Shchemelev and A. S. Shtym, “Efficiency of flat solar collectors,” 2023.
[30] N. R. Esanaliyeva, “Hot water storage heat protector,” Eurasian Journal of Academic Research, vol. 1, no. 1, pp. 36–42, 2021.
[31] S. F. Ergashev and N. R. Esanaliyeva, “Quyosh suv isitgichlari ishlab chiqarish,” AndMI Conference, pp. 233–235, 2022.
[32] R. A. Zakhidov, Tekhnologiya i ispytaniya geliotekhnicheskikh sistem. Toshkent, O‘zbekiston: Fan, 1986.
[33] J. Twidell and A. Weir, Renewable Energy Resources. Moscow, Russia: Energoizdat, 1990.
[34] K. Boybutaev, J. Murodov, and Y. Usmonov, Quyosh energiyasidan foydalanish. Toshkent, O‘zbekiston, 1964.
[35] R. R. Avezov et al., Solar Water Heaters: Scientific and Experimental Study.
[36] R. Kumar et al., “Heat transfer in solar air channel,” Renewable Energy, vol. 101, pp. 856–872, 2017.
[37] B. A. Abdukarimov and A. A. Kuchkarov, “Hydraulic resistance of solar air heaters,” Journal of Siberian Federal University, vol. 15, no. 1, pp. 14–23, 2022.
[38] B. A. Abdukarimov, Sh. R. O‘tbo‘sarov, and A. M. Abdurazakov, “Solar air heaters for drying,” E3S Web of Conferences, vol. 264, 2021.
[39] A. Malhotra, H. P. Garg, and A. Patil, “Heat loss in solar collectors,” J. Therm. Eng., vol. 2, pp. 59–62, 1981.
[40] A. S. Yadav and J. L. Bhagoria, “CFD analysis of solar air heater,” Int. J. Heat Mass Transfer, vol. 70, pp. 1016–1039, 2014.